

Heavy Hybrids from NRQCD

UKQCD COLLABORATION

T. Manke¹, I.T. Drummond², R.R. Horgan³, H.P. Shanahan⁴

DAMTP, University of Cambridge, Cambridge CB3 9EW, England

Abstract

We present a quenched lattice calculation for the lowest lying $b\bar{b}g$ -hybrid states in the framework of NRQCD using the leading order Hamiltonian up to $\mathcal{O}(mv^2)$. We demonstrate the existence of a nearly degenerate rotational band of states with an excitation energy approximately 1.6 GeV above the Υ ground state. This lies around the $B\bar{B}_J^*$ -threshold but well above the $B\bar{B}$ -threshold. Therefore a heavy hybrid signal may well be detected if the centre-of-mass energy in B-factories is raised a few hundred MeV to coincide with other resonances above the 4S state. Our prediction is consistent with most phenomenological models and lattice calculations carried out in the static limit.

1 Introduction

Hybrid mesons are of intense interest both theoretically and experimentally because of the opportunity they provide for investigating nonperturbatively the gluonic degrees of freedom in QCD. In contrast to the standard $q\bar{q}$ -mesons in which the quarks form a colour singlet, hybrids contain quarks in a colour octet state. There exist hybrid states that have quantum numbers not available to pure $q\bar{q}$ -states and as a result do not mix with them. These *exotic* states are of particular interest. Interest has been further heightened by the recently reported discovery at Brookhaven of a 1^{-+} state at $(1370 \pm 16^{+50}_{-30})$ MeV [1]. However, the experimental study of such light hybrids is made difficult by the density of levels in the 1-2 GeV range and by strong mixing effects. Such difficulties are minimised for heavy hybrids and this should result in a clearer signal at the appropriate energies in future B-factories.

The study of hybrid states has been approached in a number of ways, such as flux tube models [2], bag models [3], sum rules [4] and the constituent gluon model [5]. Light hybrids have been studied in the framework of lattice QCD [6, 7]. Heavy hybrids have been approached through the static quark limit [8] by identifying a $q\bar{q}$ -potential appropriate to each gluonic excitation [9].

In this paper we study hybrid excitations of the $b\bar{b}$ -system using NRQCD [10]. This allows us to go beyond the static limit. Our calculation is preliminary in that we use only the lowest order heavy quark Hamiltonian and employ the quenched approximation for the gluon field. Previous work confirms that this approximation gives a reasonable account of low lying spin averaged energy levels of heavy quark systems [11, 12]. In this sense we believe we have

¹T.Manke@damtp.cam.ac.uk

²itd@damtp.cam.ac.uk

³rrh@damtp.cam.ac.uk

⁴H.P.Shanahan@damtp.cam.ac.uk

achieved an acceptable computation of the lowest *magnetic* hybrid excitations. We have not yet computed the hybrid levels with opposite parity. Within bag models these *electric* hybrids are believed to lie higher in energy than the corresponding magnetic states [3].

In Section 2 we introduce the non-relativistic evolution equation for the quark propagator. In Section 3 we discuss continuum operators that connect the hybrid states to the vacuum and in Section 4 we set out the lattice versions of these operators that were used in our simulation. The results are presented in Section 5.

2 NRQCD and Heavy Quark Propagators

The NRQCD approach to the computation of the heavy quark propagator $G(x, y)$, has been explained previously [11, 12]. For completeness we record here the Euclidean time evolution equation, namely

$$G(\mathbf{x}, t + 1; y) = \left(1 - \frac{aH_0}{2n}\right)^n U_t^\dagger(x) \left(1 - \frac{aH_0}{2n}\right)^n G(\mathbf{x}, t; y) \quad , \quad t \geq t_y \quad . \quad (1)$$

The initial condition has the form

$$G(\mathbf{x}, t = t_y; y) = S(\mathbf{x}, \mathbf{y}) \quad . \quad (2)$$

where $S(\mathbf{x}, \mathbf{y})$ is the source term on the first timeslice, ($t = t_y$), appropriate to the channel under study. In this paper the Hamiltonian is

$$H_0 = -\frac{\Delta^2}{2m_b} \quad , \quad (3)$$

where m_b is the bare quark mass and Δ^2 is the standard spatial covariant Laplacian defined in [10]. In the calculation all the link variables are tadpole improved according to the replacement $U_\mu(x) \rightarrow U_\mu(x)/u_0$ where u_0 is obtained from the plaquette U_\square : $u_0 = \langle 0 | \frac{1}{3} \text{Tr} U_\square | 0 \rangle^{1/4}$. Other suggested improvements [13], make no significant difference to the present calculation which is concerned only with spin averaged quantities. This is consistent with our neglect of higher corrections to the Hamiltonian that incorporate quark spin-gluon couplings and $\mathcal{O}(mv^4)$ terms.

3 Hybrid States and Operators

We will use the standard nomenclature for hybrid states [14] in which charge conjugation and parity satisfy

$$C = (-1)^{l+s+1} \quad (4)$$

$$P = \begin{cases} (-1)^{l+j} & \text{TE} \\ (-1)^{l+j+1} & \text{TM} \end{cases} \quad , \quad (5)$$

where l and s are the $q\bar{q}$ orbital angular momentum and spin, and j is the gluon angular momentum. The historical notations TE and TM refer to the magnetic and electric hybrid states, respectively.

To extract masses we calculate two-point functions of operators with the appropriate quantum numbers. For hybrid states these operators must include a gluon field factor in

order to ensure the presence of a gluon excitation. This is done by introducing the gauge field operators

$$\begin{aligned} B_i &= \frac{1}{2}\epsilon_{ijk}F_{jk} \ , \\ E_i &= F_{it} \ , \end{aligned} \tag{6}$$

where $F_{\mu\nu}$ is the gluon field tensor. We can alternatively replace \mathbf{E} by $\nabla \times \mathbf{B}$ to access the same quantum numbers on a single timeslice.

From B_i we can construct the $j = 1$ *magnetic* hybrid operators. The spin singlet states are coupled to the vacuum by the operators defined in Table 1.

state	l	J^{PC}
$\chi^\dagger B_i \psi$	0	1^{--}
$\chi^\dagger \{B_i, D_i\} \psi$	1	0^{++}
$\chi^\dagger \epsilon_{ijk} \{B_j, D_k\} \psi$	1	1^{++}
$\chi^\dagger (\{B_i, D_j\} + \{B_j, D_i\} - \frac{1}{3}\delta_{ij} \{B_i, D_j\}) \psi$	1	2^{++}

Table 1: Continuum operators for spin-singlet hybrid states. The non-relativistic 2 spinors, ψ and χ^\dagger , denote the quark field and anti-quark field, respectively.

It has been pointed out by Griffiths *et al.* [15] that there is a common $q\bar{q}$ -potential interaction for all the $j = 1$ states in the static quark limit. The presence of excited glue, however, results in a relatively shallow structure for the radial dependence of the potential function. Consequently we can anticipate that the orbital motion of *finite* mass quarks in the presence of this potential will give rise to a nearly degenerate rotational band of states. In particular the $l = 0$ and $l = 1$ states will be approximately degenerate. If, in addition, the orbital dynamics of the quarks is controlled by a spin-independent force, as is the case in the approximation used in this paper, the triplet quark states built on the above singlet states will also lie in the same degenerate band. The triplet states shown in Table 2 are built on the 1^{--} state and contain the 1^{-+} which has exotic quantum numbers. Triplet states built

state	l	J^{PC}
$\chi^\dagger \sigma_i B_i \psi$	0	0^{-+}
$\epsilon_{ijk} \chi^\dagger \sigma_j B_k \psi$	0	1^{-+}
$\chi^\dagger (\sigma_i B_j + \sigma_j B_i - \frac{1}{3}\delta_{ij} \sigma_i B_i) \psi$	0	2^{-+}

Table 2: Continuum operators for spin-triplet states corresponding to the 1^{--} .

on the 1^{++} are shown in Table 3. Those contain also the exotics 0^{+-} and 2^{+-} . There are further triplet states including a 3^{+-} state. All these states can be expected to be essentially degenerate in the case of our simple spin-independent Hamiltonian.

state	l	J^PC
$\chi^\dagger \sigma_i \epsilon_{ijk} \{B_j, D_k\} \psi$	1	0^{+-}
$\chi^\dagger \sigma_j (\{B_i, D_j\} - \{B_j, D_i\}) \psi$	1	1^{+-}
$\chi^\dagger (\sigma_i \epsilon_{jkl} \{B_k, D_l\} + \sigma_j \epsilon_{ikl} \{B_k, D_l\} - \frac{1}{3} \delta_{ij} \sigma_i \epsilon_{jkl} \{B_k, D_l\}) \psi$	1	2^{+-}

Table 3: Continuum operators for spin-triplet states corresponding to the 1^{++} .

4 Lattice Operators

Because our evolution equation involves no spin-corrections to the Hamiltonian we focus on the lattice versions of the operators in Table 1. In constructing them we replace covariant derivatives, D_i , with covariant lattice derivatives, Δ_i^n , in the extended form used in [12, 16]. For the magnetic gluon operators which involve only spatial derivatives this presents no problem since these operators can be formulated in terms of variables on a single timeslice. We define the colour magnetic field on the lattice as

$$B_i^n = \frac{1}{2} \epsilon_{ijk} [\Delta_j^n, \Delta_k^n] \quad , \quad (7)$$

with the definition

$$\begin{aligned} \Delta_i^n \psi(x) &\equiv L_i^n \psi(x + ni) - L_{-i}^n \psi(x - ni) \\ L_i^n \psi(x) &\equiv U_i(x) U_i(x + i) \dots U_i(x + (n-1)i) \psi(x + ni) \end{aligned} \quad (8)$$

As in an earlier study [16], these operators result in commutators of extended link variables for the hybrid state

$$B_i^n = \frac{1}{2} \epsilon_{ijk} \{ [L_j^n, L_k^n] - [L_{-j}^n, L_{-k}^n] \} \quad , \quad (9)$$

For the free field case, where $U_\mu(x) = 1$, these operators vanish as expected. Finally we have the extended hybrid operator

$$H_i^n(\mathbf{x}) = \epsilon_{ijk} \chi^\dagger(\mathbf{x}) ([L_j^n, L_k^n] - [L_{-j}^n, L_{-k}^n]) \psi(\mathbf{x}) \quad . \quad (10)$$

We have achieved a significant improvement for the signal by employing the fuzzing algorithm for link variables suggested in [17]. We use a central link weight of $c = 2.5$ with six fuzzing iterations. We now use those *fuzzed* link variables to construct the extended links, which we then use in the meson operators. Phenomenological models indicate that hybrid states are more extended than the standard $q\bar{q}$ -states. This suggests that operators with large spatial separation will have the best overlaps. In compromising between spatial size of the operators and the efficiency of the code we choose $n=4$ and 5 . In some cases the operators were further improved by using, in addition, Jacobi-smearing for the quark fields [18].

The meson correlator is written as a Monte Carlo average over all configurations

$$C^{nm}(x, y) = \langle \text{tr} [G^\dagger(x, y) G^{nm}(x, y)] \rangle \quad , \quad (11)$$

O_h irrep.	$\chi^\dagger(x) O \Psi(x)$	lowest contiuum J^{PC}
A_1	1	0^{-+}
T_1	$\epsilon_{ijk} \Delta_j \Delta_k$	1^{--}
A_1	$\epsilon_{ijk} \Delta_i \Delta_j \Delta_k$	0^{++}
T_1	$\epsilon_{ijk} \epsilon_{klm} \{\Delta_j, \Delta_l \Delta_m\}$	1^{++}
T_2	$s_{ijk} \epsilon_{klm} \{\Delta_j, \Delta_l \Delta_m\}$	2^{++}
E	$S_{\alpha jk} \epsilon_{klm} \{\Delta_j, \Delta_l \Delta_m\}$	2^{++}

Table 4: Equivalent lattice operators of Table 1. The first column denotes the irreducible representation of the octahedral group. We define $s_{ijk} = |\epsilon_{ijk}|$ and $S_{\alpha jk}$ projects out the two linearly independent traceless-symmetric combinations corresponding to the representation E.

β	6.0
$L^3 \times T$	$16^3 \times 48$
a^{-1} in GeV (from $1P - 1S$)	2.44(4)
am_b, n	1.71, 2
u_0	0.878
spatial starts	8
temporal starts	5
total number of measurements	20, 000

Table 5: The parameters in our simulation. To increase the statistics, we chose several starting points per configuration.

where \mathbf{tr} denotes contraction over all internal degrees of freedom and G^{nm} is the smeared propagator defined by

$$G^{nm}(x, y) \equiv \sum_{z_1, z_2} O^n(x, z_1) G(z_1, z_2) O^{m\dagger}(z_2, y) . \quad (12)$$

Here (n, m) stands for the radii at (sink, source) and the O^n are operators as defined in Table 4. For the extended propagator we solve equation 1 with $S(\mathbf{x}, \mathbf{y}) = O^{m\dagger}(\mathbf{x}, \mathbf{y})$ and multiply with O^n at the sink. We fix the origin at some (arbitrary) lattice point, y , and sum over all spatial \mathbf{x} so as to project out the zero momentum mode.

5 Simulation and Results

The parameters of our simulation are shown in Table 5. The quenched gauge field configurations were all generated at the EPCC in Edinburgh. The propagators were calculated at the HPCF in Cambridge.

We fit the correlators to the multi-exponential form

$$C_\alpha^{mm}(t) = \sum_{i=1}^{\text{nfit}} a_{\alpha i}^{nm} e^{-M_i^\alpha t} . \quad (13)$$

Operator	State	Fit results		Energies [GeV]	
		aE_0	$aE_1 - aE_0$	$E_0 - E_\Upsilon$	$E_1 - E_0$
1	0^{-+}	0.4487(13)	–	0.	–
$\sum_i B_i$	1^{--}	1.114(40)	0.628(66)	1.62(10)	1.53(16)
$\Delta_i \cdot B_i$	0^{++}	1.175(22)	0.609(73)	1.775(61)	1.49(18)
$\{\Delta_{[i, B_j]} \rightarrow \sum_i [\Delta_i, \Delta^2]$	1^{++}	1.134(19)	0.61(10)	1.674(54)	1.49(25)
$\{\Delta_{\{1, B_2\}}\}$	$2^{++}(T_2)$	1.161(19)	0.600(61)	1.740(55)	1.47(15)
$\{\Delta_1, B_1\} - \{\Delta_2, B_2\}$	$2^{++}(E)$	1.126(13)	0.520(58)	1.655(42)	1.27(14)

Table 6: Hybrid spectrum from 499 configurations at $\beta = 6.0$, $am_b = 1.71$, $u_0 = 0.878$, $a_{1P-1S}^{-1} = 2.44(4)$ GeV. E_0 and E_1 denote the energies of ground and first excited states in the relevant channel. The results are obtained from a two-exponential fit as shown in column 3 and 4. In column 5 and 6 we have converted all results into physical units, using the inverse lattice spacing which is determined from the $1P - 1S$ splitting. The ground state in each channel is given relative to the $\Upsilon(1S)$.

Here α denotes a meson state with certain quantum numbers, (n, m) the different radii at the (sink, source) and t the Euclidean time. As the hybrid excitations are very high above the ground state the signal-to-noise ratio deteriorates very quickly and vanishes at $t \gtrsim 15$. Therefore we choose $t_{\max} = 12$ and vary t_{\min} in search of a plateau. An example of such a plot for the lowest lying $b\bar{b}$ -hybrid is shown in Figure 1. A collection of our results can be found in Table 6 and Figure 2.

We quote the masses from plateaus where $\chi^2/\text{dof} < 1$. The error estimate is calculated from the inverse of the Hessian matrix which is determined during a Levenberg-Marquardt χ^2 minimisation [19].

6 Conclusions

In this paper we reported on a heavy hybrid signal obtained within the framework of NRQCD. This field theoretical calculation goes beyond the static approximation and so has the virtue of incorporating the dynamics of the heavy quarks. In our investigation we calculated the masses of hybrids where the $q\bar{q}$ -pair is in a colour octet coupled to the colour magnetic field. Some of the results have already been reported elsewhere [20]. Work on the same configurations using different operators has been discussed in [21]. We obtained a signal for several correlation functions where the magnetic field couples to spin-singlet states of different orbital angular momenta, as listed in Table 4. Static potential models predict that the above states should lie in a nearly degenerate rotational band. From Table 6 and Figure 2 it can be seen that our results confirm this picture to within two standard deviations. For our Hamiltonian all the spin-triplet states are degenerate in energy with the spin-singlets and we are only sensitive to spin-averaged quantities. Therefore, the exotic 1^{-+} state is degenerate in this approximation with the 1^{--} and likewise both the 0^{+-} and 2^{+-} are degenerate with the 1^{++} .

Phenomenologically, there are two important thresholds for the production and decay of hybrid $b\bar{b}$ -states. These are the $B\bar{B}$ -threshold at 10.56 GeV and the $B\bar{B}_J^*$ -threshold at 11.01 GeV. For the latter we assume that $B_J^*(5732)$ is indeed a P-wave as suggested in the Particle

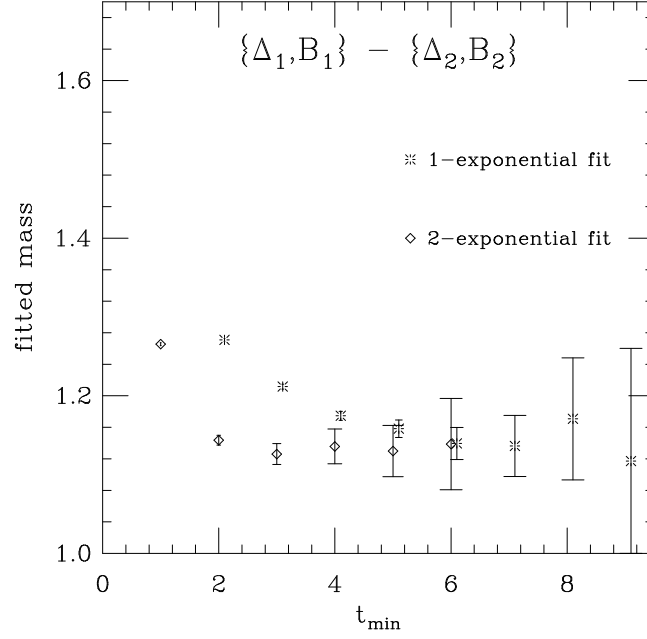


Figure 1: Fit to hybrid signal. Consistent fit results are shown for the ground state for both a 1-exponential fit and a 2-exponential fit.

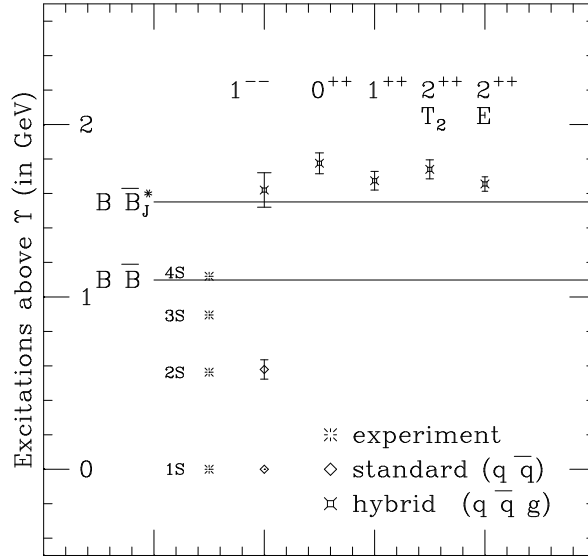


Figure 2: Results. The 1^{--} is 1.62(10) GeV above the 1S. The corresponding rotational band appears to be degenerate around the $B\bar{B}_J^*$ -threshold. Each state is the spin-averaged and some of them contain also the exotics $1^{-+}, 0^{+-}, 2^{+-}$. See main text.

Data Book [22]. Sometimes this state is also referred to as B^{**} . Below the (S+P)-threshold hybrid states are thought to be stable [23]. As can be seen from Figure 2 our results suggest that hybrid states lie close to the (S+P)-threshold and 4-5 standard deviations above the (S+S)-threshold.

In our calculation there are a number of sources of systematic errors. First, we have retained only terms $\mathcal{O}(mv^2)$ in the Hamiltonian and neglected those $\mathcal{O}(mv^4)$ and higher. Numerically this may not be a bad approximation since we expect the quarks in the hybrid states to be even more non-relativistic than in the Υ itself. This is consistent with the very shallow $q\bar{q}$ -potential predicted in the static limit of the hybrid state [8, 24, 25] and the implied near degeneracy of the resulting rotational band - a result confirmed in our calculation. However a study of singlet-triplet splitting requires that higher order terms, such as $\sigma \cdot \mathbf{B}$, be taken into account. The above argument suggests that this splitting is small. Furthermore, there may be finite size effects because the hybrids in the shallow potential are expected to be larger than the Υ . From studies in the static limit one expects the interquark separation in $b\bar{b}g$ to be of the order of 0.5 fm [21, 25]. The actual extent of a hybrid state may still be bigger than this [3]. We note that for the parameters used in this paper the lattice has a spatial extent of approximately 1.3 fm.

Finally, and perhaps most importantly, we must take into account uncertainties in the value of a^{-1} , the inverse lattice spacing. These uncertainties are intrinsic to any calculation based on a quenched gluon approximation, since not all mass ratios can be simultaneously correct. The result therefore depends on which observables are used to fit a^{-1} . In the numbers quoted above we used the $1P - 1S$ mass difference of a standard NRQCD calculation of the Υ -system. This is a consistent approach and yields $a^{-1} = 2.44(4)$ GeV and our number of 11.08(10) GeV for the lowest hybrid. Perantonis and Michael quote 10.81(25) GeV from a Schrödinger Equation using the static potential from the lattice, where a_σ^{-1} is determined from the string tension in the quenched approximation [8]. Their error also includes an estimate for quenching effects. If we use their value of $a_\sigma^{-1} = 2.04(2)$ GeV, we obtain the mass of the 1^{-+} to be 10.82(8) GeV, which is consistent with their result. These uncertainties should be resolved in a simulation with dynamical light quarks where the coupling runs appropriately and the inverse lattice spacing is expected to be the same when determined at different scales. Therefore the issue whether the hybrid states lie above or below the $B\bar{B}^*$ -threshold, must be addressed using unquenched gauge field configurations. Subject to this uncertainty in the value of the inverse lattice spacing, our results are consistent with the predictions from most phenomenological models [26].

Acknowledgements

We would like to thank other members of the UKQCD collaboration in particular S. Collins for useful discussions. T.M. is supported by a grant from EPSRC (Ref. No. 94007885). H.P.S. is supported by the Leverhulme Trust. Our calculations are performed on the Hitachi SR2001 located at the University of Cambridge High Performance Computing Facility and the CRAY-T3D at the Edinburgh Parallel Computing Centre at Edinburgh University.

References

- [1] D.R. Thompson *et al.* Phys. Rev. Lett. 79, (1997), 1630-1633.

- [2] N. Isgur and J. Paton, Phys. Rev. **D31**, (1985), 2910-2929.
- [3] P. Hasenfratz *et al.*, Phys. Lett. **B95**, (1981), 299-305.
T. Barnes *et al.*, Nucl. Phys. **B224**, (1983), 241-264.
- [4] J. Govaerts *et al.*, Nucl. Phys. **B284**, (1987), 674-689.
- [5] Yu.S. Kalashnikova and Yu.B. Yufryakov, Phys.Atom.Nucl.60, (1997), 307-313
- [6] P. Lacock *et al.*, UKQCD Collaboration, Phys. Rev. **D54**, (1996), 6997-7009.
- [7] C. Bernard *et al.*, MILC Collaboration, Nucl. Phys. **B** (Proc. Suppl.) **53**, (1997), 228-230.
C. Bernard *et al.*, MILC Collaboration, hep-lat/9707008.
- [8] S. Perantonis and C. Michael, Nucl. Phys. **B347**, (1990), 854-868.
- [9] I.J. Ford *et al.*, Phys. Lett. **B208**, (1988), 286-290.
- [10] G.P. Lepage *et al.*, Phys. Rev. **D46**, (1992), 4052-4067.
- [11] C.T.H. Davies *et al.* Phys. Rev. **D50**, (1994), 6963-6977.
- [12] T. Manke *et al.*, UKQCD Collaboration, Phys. Lett. **B408**, (1997), 308-314.
- [13] H.D. Trottier, Phys. Rev. **D55**, (1997), 6844-6851.
- [14] A. Le Yaouanc *et al.*, Z. Phys. **C28**, (1985), 309-315.
- [15] L.A. Griffiths *et al.*, Phys. Lett. **B129**, (1983), 351-356.
- [16] S. Catterall *et al.*, UKQCD Collaboration, Phys. Lett. **B300**, (1993), 393-399.
- [17] P. Lacock *et al.*, UKQCD Collaboration, Phys. Rev. **D51**, (1995), 6403-6410.
- [18] C.R. Allton *et al.*, UKQCD Collaboration, Phys. Rev. **D47**, (1993), 5128-5137.
- [19] W.H. Press *et al.*, "Numerical recipes in Fortran", (2nd Edition), Cambridge University Press (1992).
- [20] T. Manke *et al.*, UKQCD Collaboration, to appear in Nucl. Phys. **B** (Proc. Suppl), proceedings of Lattice '97, Edinburgh, hep-lat/9709001.
- [21] S. Collins *et al.*, UKQCD Collaboration, to appear in Nucl. Phys. **B** (Proc. Suppl), proceedings of Lattice '97, Edinburgh, hep-lat/9710058.
- [22] R.M. Barnett *et al.*, Phys. Rev. **D54**, (1996), 1.
- [23] F. E. Close and P. R. Page, Nucl. Phys. **B443**, (1995), 233-254.
- [24] K.J. Juge *et al.*, to appear in Nucl. Phys. **B** (Proc. Suppl), proceedings of Lattice '97, Edinburgh, hep-lat/9709132.
- [25] K.J. Juge *et al.*, to appear in Nucl. Phys. **B** (Proc. Suppl), proceedings of Lattice '97, Edinburgh, hep-lat/9709131.
- [26] T. Barnes *et al.*, Phys. Rev. **D52**, (1995), 5242-5256.